J|A|C|S ARTICLES

Published on Web 12/29/2009

Persistent, Well-Defined, Monodisperse, π-Conjugated Organic Nanoparticles *via* G-Quadruplex Self-Assembly

David González-Rodríguez,*,† Pim G. A. Janssen,‡ Rafael Martín-Rapún,‡ Inge De Cat,§ Steven De Feyter,*,§ Albertus P. H. J. Schenning,*,‡ and E. W. Meijer*,‡,||

Departamento de Química Orgánica, Facultad de Ciencias, Universidad Autónoma de Madrid, E-28049 Madrid, Spain, Laboratory for Macromolecular and Organic Chemistry, Eindhoven University of Technology, 5600 MB Eindhoven, The Netherlands, and Division of Molecular and Nanomaterials, Laboratory of Photochemistry and Spectroscopy, and Institute of Nanoscale Physics and Chemistry, Katholieke Universiteit Leuven, B-3001, Leuven, Belgium

Received October 14, 2009; E-mail: david.gonzalez.rodriguez@uam.es; a.p.h.j.schenning@tue.nl; e.w.meijer@tue.nl; steven.defeyter@chem.kuleuven.be

Abstract: Several oligo(*p*-phenylene-vinylene) oligomers capped with a guanosine or a guanine moiety have been prepared *via* a palladium-catalyzed cross-coupling reaction. Their self-assembly, in both the absence and presence of alkaline salts, has been studied by means of different techniques in solution (NMR, MS, UV−vis, CD, fluorescence), solid state (X-ray diffraction), and on surfaces (STM, AFM). When no salt is added, these π-conjugated molecules self-associate in a mixture of hydrogen-bonded oligomers, among which the G-quartet structure may be predominant if the steric hindrance around the guanine base becomes important. In contrast, in the presence of sodium or potassium salts, well-defined assemblies of eight functional molecules (8mers) can be formed selectively and quantitatively. In these assemblies, the π-conjugated oligomers are maintained in a chirally tilted (J-type) stacking arrangement, which is manifested by negative Cotton effects, small bathochromic absorption and emission shifts, and fluorescence enhancements. Furthermore, these self-assembled organic nanostructures, ~1.5−2.0 nm high and 8.5 nm wide, exhibit an extraordinary stability to temperature or concentration changes in apolar media, and they can be transferred and imaged over solid substrates as individual nanoparticles, showing no significant dissociation or further aggregation.

Introduction

The successful development of nanosized technologies relies on the ability of researchers to efficiently manufacture persistent structures of nanometer dimensions that are endowed with a particular function. Within this context, organic nanoparticles (ONPs) have become the subject of increasing attention in the past years.[1] In addition to their current use in inks, drugs, or cosmetics, they are promising materials for optoelectronics,[2] semiconductors,[3] and biological sensing[4] applications. Compared to inorganic semiconductor or metal nanoparticles, ONPs enjoy a much wider structural versatility, due to their diversity in molecular constitution and arrangement, their higher biocompatibility, and a more flexible material preparation. However, the conventional techniques for producing ONPs[1,5] allow limited control on particle size and distribution (usually >20 nm) as well as on the relative arrangement of the molecular components. These are key issues that determine many properties of the nanostructures. Similar to their inorganic counterparts, the special properties of ONPs, lying between those of individual molecules and bulk materials, exhibit confinement effects caused by their finite size.[3,6] For instance, recent studies have shown a size-dependent enhancement of fluorescence emission,[4,7] which is believed to have its origin in the stacking arrangement within the ONP. On one hand, aggregation causes a significant planarization of the molecules, and nonradiative decays are reduced due to a restricted conformational motion. On the other hand, some intermolecular orientations lead to J-type aggregates that display bathochromic absorption and enhanced, red-shifted emission features.[4,7a,c,d]

† Universidad Autónoma de Madrid.
‡ Laboratory for Macromolecular and Organic Chemistry, Eindhoven University of Technology.
§ Katholieke Universiteit Leuven.
|| Present address: Institute for Complex Molecular Systems, Eindhoven University of Technology, P.O. Box 513, 5600 MB Eindhoven, The Netherlands.

(1) Horn, D.; Rieger, J. *Angew. Chem., Int. Ed.* **2001**, *40*, 4330–4361.
(2) (a) Lim, S.-J.; An, B.-K.; Jung, S. D.; Chung, M.-A.; Park, S. Y. *Angew. Chem., Int. Ed.* **2004**, *43*, 6346–6350. (b) An, B.-K.; Kwon, S.-K.; Park, S. Y. *Angew. Chem., Int. Ed.* **2007**, *46*, 1978–1982.
(3) Wang, F.; Han, M.-Y.; Mya, K. Y.; Wang, Y.; Lai, Y.-H. *J. Am. Chem. Soc.* **2005**, *127*, 10350–10355.
(4) Kim, H.-J.; Lee, J.; Kim, T.-H.; Lee, T. S.; Kim, J. *Adv. Mater.* **2008**, *20*, 1117–1121.
(5) ONPs can be prepared by rapid expansion of supercritical solutions (see ref 5a), stabilization by surfactants (refs 5b,5c), laser ablation of microcrystals (ref 5d), or by the most common reprecipitation method (see refs 6,7). (a) Sane, A.; Thies, M. C. *J. Phys. Chem. B* **2005**, *109*, 19688–19695. (b) Kang, L.; Wang, Z.; Cao, Z.; Ma, Y.; Fu, H.; Yao, J. *J. Am. Chem. Soc.* **2007**, *129*, 7305–7312. (c) Dang, Z.-M.; Gao, Y.; Xu, H.-P.; Bai, J. *J. Colloid Interface Sci.* **2008**, *322*, 491–496. (d) Asahi, T.; Sugiyama, T.; Masuhara, H. *Acc. Chem. Res.* **2008**, *41*, 1790–1798.
(6) Fu, H.-B.; Yao, J.-N. *J. Am. Chem. Soc.* **2001**, *123*, 1434–1439.

 10.1021/ja908537k

Molecular self-assembly[8] offers an excellent alternative tool to cheaply and easily construct, *via* a "Bottom-Up" approach, diverse supramolecular architectures smaller than 100 nm in which the morphology and the relative organization of individual molecules can be controlled by rational selection of different self-assembling motifs.[9] This supramolecular approach often fails, however, in providing nanostructures that are monodisperse and persistent in size and shape. Many noncovalent interactions, such as $\pi-\pi$ stacking or solvophobic interactions, promote supramolecular polymerizations,[10] and size control is generally complex to achieve. In addition, the weak nature of the noncovalent interactions that hold the molecular building blocks together make these self-assembled architectures very sensitive to concentration and temperature variations, which affects dramatically their homogeneity. The supramolecular synthesis of discrete, uniform, stable nanoobjects[11] is therefore a challenging objective that must be addressed for practical applications, so that the physical properties can be related to individual well-defined assemblies and the molecular organization is not altered upon deposition and manipulation over solid substrates.[12]

In this context, recent studies have disclosed the singular characteristics of guanine (G) self-assembly in the presence of alkaline salts,[13] where multiple noncovalent interactions (i.e., hydrogen-bonding, $\pi-\pi$ stacking and cation−dipole interactions) can work in concert to provide discrete[14−16] and relatively stable[16,17] G-quadruplexes (see Figure 1a). We and other research groups have therefore considered the G-quadruplex structure as an ideal scaffold to which photoactive organic molecules can be attached to construct functional assemblies.[18,19] Recently, the equilibrium between linear G-oligomers (G-ribbons)[20] and G-quadruplex species has been studied in porphyrin-G,[19a] pyrene-G,[19b] or oligothiophene-G[19c] conjugates. Upon addition of sodium or potassium salts, this equilibrium is

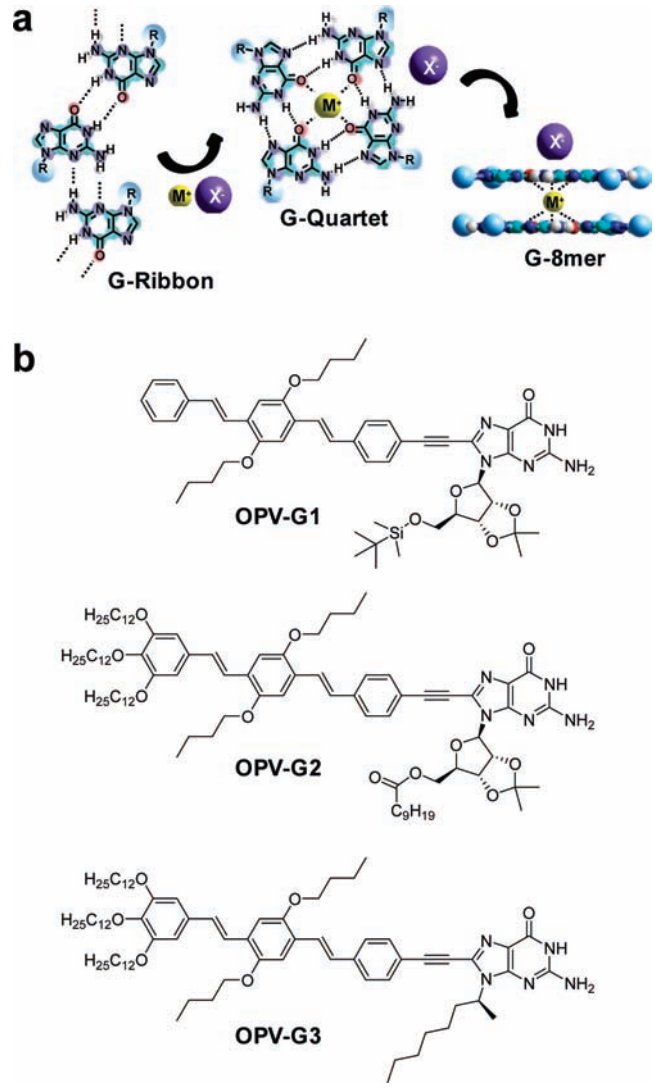

Figure 1. (a) Levels of organization in the formation of a G-quadruplex (8mer). In a first level of organization, a tetramer (G-quartet) is formed by a circular array of eight self-complementary hydrogen bonds. This arrangement leaves the four carbonyl dipolar groups pointing toward a small central cavity in which a cation can be strongly complexed. Complexation is even more efficient if another quartet layer is added on top, so the cation is now coordinated to the eight carbonyl groups of two $\pi-\pi$ stacked G-quartets whereas the anion is left out at the complex periphery. (b) Structure of the three oligophenylenevinylene-guanine (**OPV-G**) molecules studied in this work.

(7) (a) An, B.-K.; Kwon, S.-K.; Jung, S.-D.; Park, S. Y. *J. Am. Chem. Soc.* **2002**, *124*, 14410–14415. (b) Xiao, D.; Xi, L.; Yang, W.; Fu, H.; Shuai, Z.; Fang, Y.; Yao, J. *J. Am. Chem. Soc.* **2003**, *125*, 6740–6745. (c) Li, S.; He, H.; Xiong, F.; Li, Y.; Yang, G. *J. Phys. Chem. B* **2004**, *108*, 10887–10892. (d) Bhongale, C. J.; Chang, C.-W.; Lee, C.-S.; Diau, E. W.-G.; Hsu, C.-S. *J. Phys. Chem. B* **2005**, *109*, 13472–13482. (e) Sun, Y.-Y.; Liao, J.-H.; Fang, J.-M.; Chou, P.-T.; Schen, C.-H.; Hsu, C.-W.; Chen, L.-C. *Org. Lett.* **2006**, *8*, 3713–3716. (f) Ou, Z.; Yao, H.; Kimura, K. *J. Photochem. Photobiol. A* **2007**, *189*, 7–14. (g) Palayangoda, S. S.; Cai, X.; Adhikari, R. M.; Neckers, D. C. *Org. Lett.* **2008**, *10*, 281–284. (h) Yao, H.; Yamashita, M.; Kimura, K. *Langmuir* **2009**, *25*, 1131–1137. (i) Adhikari, R. M.; Shah, B. K.; Palayangoda, S. S.; Neckers, D. C. *Langmuir* **2009**, *25*, 2402–2406.
(8) Whitesides, G. M.; Grzybowski, B. *Science* **2002**, *295*, 2418–2421.
(9) (a) Janssen, P. G. A.; Jabbari-Farouji, S.; Surin, M.; Vila, X.; Gielen, J. C.; de Greef, T. F. A.; Vos, M. R. J.; Bomans, P. H. H.; Sommerdijk, N. A. J. M.; Christianen, P. C. M.; Leclère, Ph.; Lazzaroni, R.; van der Schoot, P.; Meijer, E. W.; Schenning, A. P. H. J. *J. Am. Chem. Soc.* **2009**, *131*, 1222–1232. (b) Janssen, P. G. A.; Ruiz-Carretero, A.; González-Rodríguez, D.; Meijer, E. W.; Schenning, A. P. H. J. *Angew. Chem., Int. Ed.* **2009**, *48*, 8103–8106. (c) For a general review see: Hoeben, F. J. M.; Jonkheijm, P.; Meijer, E. W.; Schenning, A. P. H. J. *Chem. Rev.* **2005**, *105*, 1491–1546.
(10) (a) Ciferri, A. *Macromol. Rapid Commun.* **2002**, *23*, 511–529. (b) Brunsveld, L.; Folmer, B. J. B.; Meijer, E. W.; Sijbesma, R. P. *Chem. Rev.* **2001**, *101*, 4071–4098. (c) de Greef, T. F. A.; Meijer, E. W. *Nature* **2008**, *453* (7192), 171–173.
(11) Schmittel, M.; Kalsani, V. *Top. Curr. Chem.* **2005**, *245*, 1–53.
(12) Jonkheijm, P.; Hoeben, F. J. M.; Kleppinger, R.; van Herrikhuyzen, J.; Schenning, A. P. H. J.; Meijer, E. W. *J. Am. Chem. Soc.* **2003**, *125*, 15941–15949.
(13) (a) Davis, J. T. *Angew. Chem., Int. Ed.* **2004**, *43*, 668–698. (b) Davis, J. T.; Spada, G. P. *Chem. Soc. Rev.* **2007**, *36*, 296–313.
(14) (a) Forman, S. L.; Fettinger, J. C.; Pieraccini, S.; Gottarelli, G.; Davis, J. T. *J. Am. Chem. Soc.* **2000**, *122*, 4060–4067. (b) Shi, X.; Fettinger, J. C.; Davis, J. T. *J. Am. Chem. Soc.* **2001**, *123*, 6738–6739. (c) Shi, X.; Mullaugh, K. M.; Fettinger, J. C.; Jiang, Y.; Hofstadler, S. A.; Davis, J. T. *J. Am. Chem. Soc.* **2003**, *125*, 10830–10841. (d) Ma, L.; Iezzi, M.; Kaucher, M. S.; Lam, Y.-F.; Davis, J. T. *J. Am. Chem. Soc.* **2006**, *128*, 15269–15277.
(15) (a) García-Arriaga, M.; Hobley, G.; Rivera, J. M. *J. Am. Chem. Soc.* **2008**, *130*, 10492–10493. (b) Betancourt, J. E.; Martín-Hidalgo, M.; Gubala, V.; Rivera, J. M. *J. Am. Chem. Soc.* **2009**, *131*, 3186–3188.
(16) González-Rodríguez, D.; van Dongen, J. L. J.; Lutz, M.; Spek, A. L.; Schenning, A. P. H. J.; Meijer, E. W. *Nat. Chem.* **2009**, *1*, 151–155.
(17) The impressive thermodynamic and kinetic stability of this kind of assemblies has already been evidenced in a number of papers. See refs 14c−d, 16, and: (a) Davis, J. T.; Kaucher, M. S.; Kotch, F. W.; Iezzi, M. A.; Clover, B. C.; Mullaugh, K. M. *Org. Lett.* **2004**, *6*, 4265–4268. (b) Kaucher, M. S.; Lam, Y.-F.; Pieraccini, S.; Gottarelli, G.; Davis, J. T. *Chem.—Eur. J.* **2005**, *11*, 164–173.
(18) Lena, S.; Masiero, S.; Pieraccini, S.; Spada, G. P. *Chem.—Eur. J.* **2009**, *15*, 7792–7806.
(19) (a) Masiero, S.; Gottarelli, G.; Pieraccini, S. *Chem. Commun.* **2000**, 1995–1996. (b) Martic, S.; Liu, X.; Wang, S.; Wu, G. *Chem.—Eur. J.* **2008**, *14*, 1196–1204. (c) Spada, G. P.; Lena, S.; Masiero, S.; Pieraccini, S.; Surin, M.; Samorì, S. *Adv. Mater.* **2008**, *20*, 2433–2438.

Scheme 1. Synthesis of the Three OPV-G Molecules Studied in This Work and Their Precursors[a]

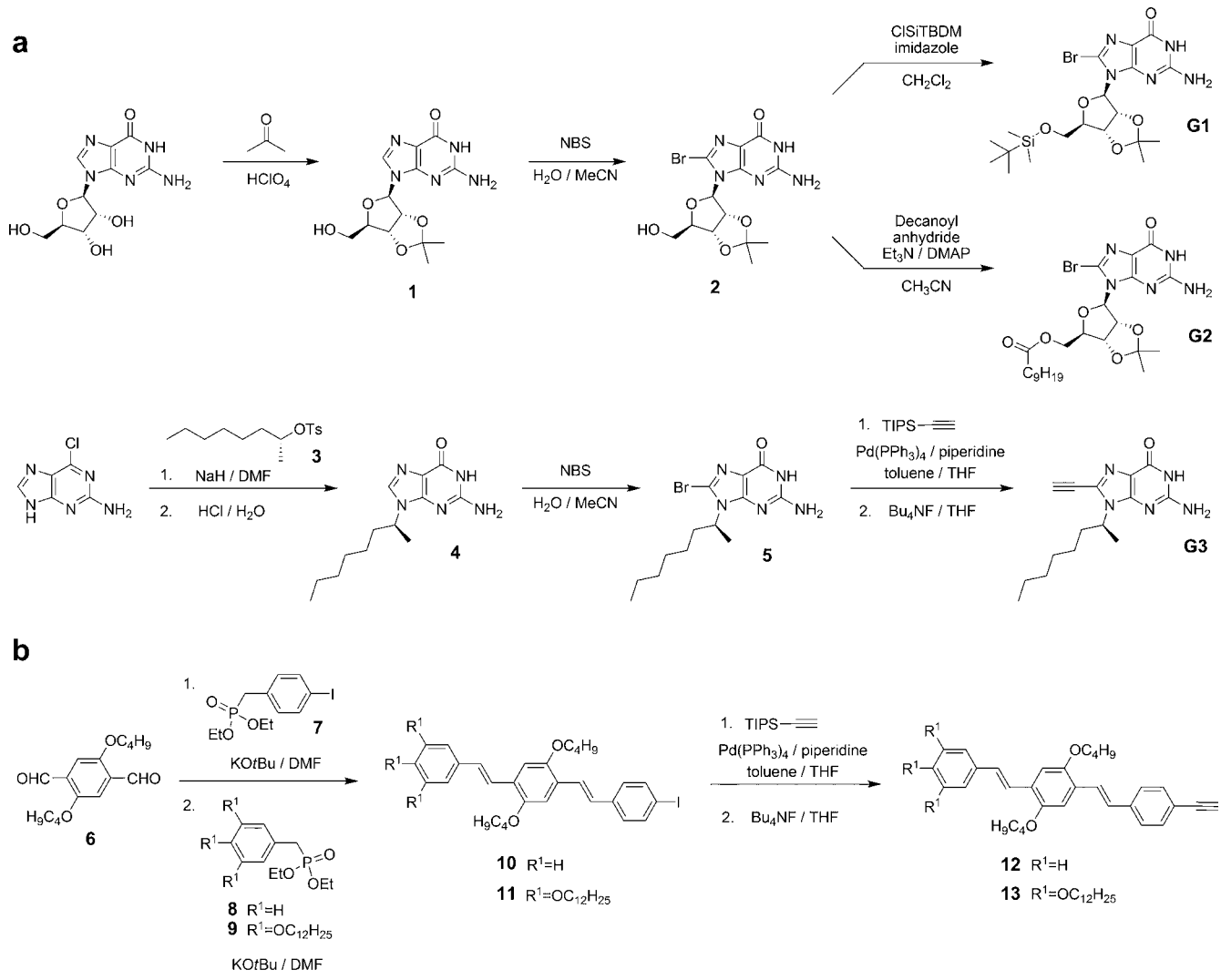

[a] (a) Synthesis of 8-bromoguanosines **G1** and **G2** and 8-ethynylguanine **G3**. (b) Synthesis of the OPV core precursors (**10**−**13**). (c) Cross-coupling reaction between the G and the OPV precursors.

shifted toward the formation of quadruplexes (typically octamers (8mers)) due to the high affinity of the stacked quartets to coordinate the cations.

Here we demonstrate not only that this approach can provide selectively and quantitatively well-defined assemblies of eight functional molecules but also that the discrete ONPs formed, ∼1.5−2.0 nm high and 8.5 nm wide, exhibit an extraordinary uniformity and stability toward temperature or concentration changes in apolar media. As a result, they can be transferred and studied over solid substrates as single entities, showing no significant dissociation or further intermolecular stacking into larger objects. In particular, we focused on the study of the self-assembly, in the absence and presence of alkaline salts, of oligo(*p*-phenylene-vinylene) (OPV), well-known semiconducting and fluorescent π-conjugated oligomers that are linked to a guanine or guanosine base (Figure 1b). The rigid nature of the ethynyl spacer employed is essential to transmit a defined orientation to the stacked OPV units in the octameric assemblies, which is mainly determined by the guanine-cation coordination. The OPVs are therefore maintained in a chirally tilted (J-type) stacking arrangement, which is manifested by negative Cotton effects, small bathochromic absorption and emission shifts, and enhancement of the fluorescence in the ONPs.

Results and Discussion

Synthesis. The synthesis of the three OPV-G compounds (Scheme 1) was envisaged via a convergent approach that involved a palladium-catalyzed Sonogashira coupling of the conjugated oligomer and the base. The latter unit contains most of the information for the self-assembly process, including the array of hydrogen-bonding groups and the chiral center.

The preparation of bromoguanines **G1**, **G2**, and **5** required two different synthetic routes (Scheme 1a). Bromoguanosines **G1** and **G2**[16] were prepared from guanosine *via* protection of the diol moiety as an acetonide,[21] bromination at the 8-position of the guanine in the presence of NBS,[22] and functionalization of the 5′-OH in the ribose with a *tert*-butyldimethylsilyl[14a,23] (**G1**) or a decanoyl[24] (**G2**) group. Compound **5** was in contrast prepared from commercial 2-amino-6-chloropurine by an N-alkylation reaction[25] with (−)-2-octyl-*p*-toluenesulfonate (**3**),[26] followed by hydrolysis[25] and subsequent bromination at the 8-position.[22] Compound **5** was then transformed to the 8-ethynyl derivative **G3** by Sonogashira coupling[27] with triisopropylsilyl acetylene and deprotection of the silyl group in the presence of tetrabutylammonium fluoride.

The synthesis of the conjugated OPV core (Scheme 1b) started from dialdehyde **6**,[28] which was subjected to a Horner−Wadsworth−Emmons reaction, first with 1.1 equiv of phosphonate **7**[29] and then with either commercial phosphonate **8** or with tridodecyloxy-phosphonate **9**.[30] This procedure led to the corresponding unsymmetrically substituted iodo-OPVs **10** and **11** in acceptable yields. Ethynyl derivatives **12** and **13** were then synthesized from **10** and **11**, respectively, by Sonogashira coupling with triisopropylsilyl acetylene and subsequent deprotection of the silyl group.

The final key step, the coupling of the chromophore and base units (Scheme 1c), was carried out using a copper-free Sonogashira procedure[27] in the presence of catalytic amounts of $Pd(PPh_3)_4$ and under strictly oxygen-free conditions, to minimize the formation of the corresponding homocoupling products. The formation of these diacetylene byproducts was still quite difficult to avoid for alkoxy-OPV **13**, especially when the coupling was performed with the rather insoluble bromoguanine **5**. Therefore, the coupling strategy was inverted for **OPV-G3**, with the reaction between ethynyl-guanine **G3** and iodo-OPV **11** leading to higher yields. All compounds were purified and characterized by ^1H and ^{13}C NMR techniques, mass spectrometry, and UV−vis and IR spectroscopies (see the Supporting Information).

Self-Assembly in the Absence of Cations. Solution Experiments. Among the natural nucleobases, guanosine certainly occupies a central role due to its versatile supramolecular chemistry. The G base offers a rich array of hydrogen-bonding donor and acceptor groups that has been exploited both by nature and by synthetic chemists to build diverse supramolecular architectures.[13] In the absence of some specific additives (alkaline cations, cytosine derivatives, ...) guanine tends to self-associate into multiple oligomeric species by formation of pairs of self-complementary hydrogen bonds (some representative examples are shown in Figure 2a). Depending on the participating hydrogen bonds, the resulting oligomers can be linear (ribbons) or circular (quartets). Although in some conditions the formation of empty quartets[31] or a particular kind of ribbon[20] is favored in concentrated samples (principally due to steric effects), the weak nature of these pairs of hydrogen bonds typically produces a complex mixture of loosely bound, rapidly exchanging oligomeric species in dilute nonpolar solutions at room temperature.

Our OPV-G compounds are quite soluble in solvents of medium-low polarity such as THF, $CHCl_3$, CH_2Cl_2, or toluene and, in the case of **OPV-G2** and **OPV-G3**, in apolar solvents such as methylcyclohexane or dodecane. ^1H NMR experiments in such solvents indicate that, like their guanosine precursors,[16] these OPV-G molecules self-associate in a mixture of oligomeric species in the absence of alkaline cations. The degree of self-association is clearly evidenced in the amide (NH) and amine (NH_2) proton signals, which shift downfield when decreasing the solvent polarity (Figure S1), the temperature (Figure 2b), or when increasing the concentration, as a result of a higher participation in hydrogen-bonding. At the same time, ESI Q-TOF MS analysis of $CHCl_3$ solutions of **OPV-G1** showed several peaks that correspond to cluster ions of the general formula $[\textbf{OPV-G1}_n+H_x(+Na_y)]^{(x+y)+}$.

Compound **OPV-G3**, which bears a guanine substituent, clearly exhibits a much higher tendency to self-associate than compounds **OPV-G1** or **OPV-G2**, substituted with a guanosine derivative. For instance, 10^{-2} M solutions of **OPV-G3** in $CDCl_2CDCl_2$, or in more apolar solvents like toluene-d_8 or cyclohexane-d_{12}, display the aforementioned downfield shift of the NH and NH_2 proton signals and a very pronounced broadening of all proton signals (Figure S2), which is attributed to the formation of ribbon-like aggregates. Such aggregation is prevented in $CDCl_2CDCl_2$ at high temperatures (>50 °C), upon addition of small amounts of CD_3OD, or using more polar solvents, such as THF-d_8 (Figure S2). On the contrary, compounds **OPV-G1** or **OPV-G2** display in general much sharper features in the ^1H NMR spectra, indicating a lower degree of aggregation. In agreement with this interpretation, DOSY experiments at 25 °C yielded comparable diffusion values for **OPV-G1** or **OPV-G2** 10^{-2} M $CDCl_3$ solutions ($D = (6.91 \pm 0.05) \times 10^{-10}$ m^2 s^{-1} and $(6.42 \pm 0.04) \times 10^{-10}$ m^2 s^{-1}, respectively), whereas somewhat lower values were observed for **OPV-G3** under the same conditions ($D = (3.89 \pm 0.09) \times 10^{-10}$ m^2 s^{-1}).

The lower tendency of **OPV-G1** or **OPV-G2** to form oligomeric aggregates, when compared to **OPV-G3**, is attributed to the larger steric volume of the ribose substituent. It is known that, in the case of 8-substituted guanosines, the ribose unit is forced to adopt a *syn* conformation, which prevents the

(20) (a) Gottarelli, G.; Masiero, S.; Mezzina, E.; Pieraccini, S.; Rabe, J. P.; Samorì, P.; Spada, G. P. *Chem.—Eur. J.* **2000**, *6*, 3242–3248. (b) Giorgi, T.; Grepioni, F.; Manet, I.; Mariani, P.; Masiero, S.; Mezzina, E.; Pieraccini, S.; Saturni, L.; Spada, G. P.; Gottarelli, G. *Chem.—Eur. J.* **2002**, *8*, 2143–2152. (c) Lena, S.; Brancolini, G.; Gottarelli, G.; Mariani, P.; Masiero, S.; Venturini, A.; Palermo, V.; Pandoli, O.; Pieraccini, S.; Samorì, P.; Sapada, G. P. *Chem.—Eur. J.* **2007**, *13*, 3757–3764.
(21) Zhang, B.; Cui, Z.; Sun, L. *Org. Lett.* **2001**, *3*, 275–278.
(22) Amer, M. S.; Amer, A. M.; Ahmed, A. F. S.; Farouk, W. M. *Indian J. Chem., Sect. B* **2001**, *40B*, 382–385.
(23) Kaucher, M. S.; Davis, J. T. *Tetrahedron Lett.* **2006**, *47*, 6381–6384.
(24) Manet, I.; Francini, L.; Masiero, S.; Pieraccini, S.; Spada, G. P.; Gottarelli, G. *Helv. Chim. Acta* **2001**, *84*, 2096–2107.
(25) (a) Norman, T. C.; Gray, N. S.; Koh, J. T.; Schultz, P. *J. Am. Chem. Soc.* **1996**, *118*, 7430–7431. (b) ElHaïk, J.; Pask, C. M.; Kilner, C. A.; Halcrow, M. A. *Tetrahedron* **2007**, *63*, 291–298.
(26) (a) Catalano, D.; Chiezzi, L.; Domenici, V.; Geppi, M.; Veracini, C. A. *J. Phys. Chem. B* **2003**, *107*, 10104–10113. (b) Elhaïk, J.; Pask, C. M.; Kilner, C. A.; Halcrow, M. A. *Tetrahedron* **2007**, *63*, 291–298.
(27) Chinchilla, R.; Nájera, C. *Chem. Rev.* **2007**, *107*, 874–922.
(28) Kuhnert, N.; López-Periago, A.; Rossignolo, G. M. *Org. Biomol. Chem.* **2005**, *3*, 524–537.
(29) Xiao, J.; Li, J.; Li, C.; Huang, C.; Li, Y.; Cui, S.; Wang, S.; Liu, H. *Tetrahedron Lett.* **2008**, *49*, 2656–2660.
(30) (a) Jonkheijm, P.; Fransen, M.; Schenning, A. P. H. J.; Meijer, E. W. *J. Chem. Soc., Perkin Trans. 2* **2001**, 1280–1286. (b) Figueira-Duarte, T. M.; Clifford, J.; Amendola, V.; Gegout, A.; Olivier, J.; Cardinali, F.; Meneghetti, M.; Armaroli, N.; Nierengarten, J.-F. *Chem. Commun.* **2006**, 2054–2056.
(31) Sessler, J. L.; Sathiosatham, M.; Doerr, K.; Lynch, V.; Abboud, K. A. *Angew. Chem., Int. Ed.* **2000**, *39*, 1300–1303.

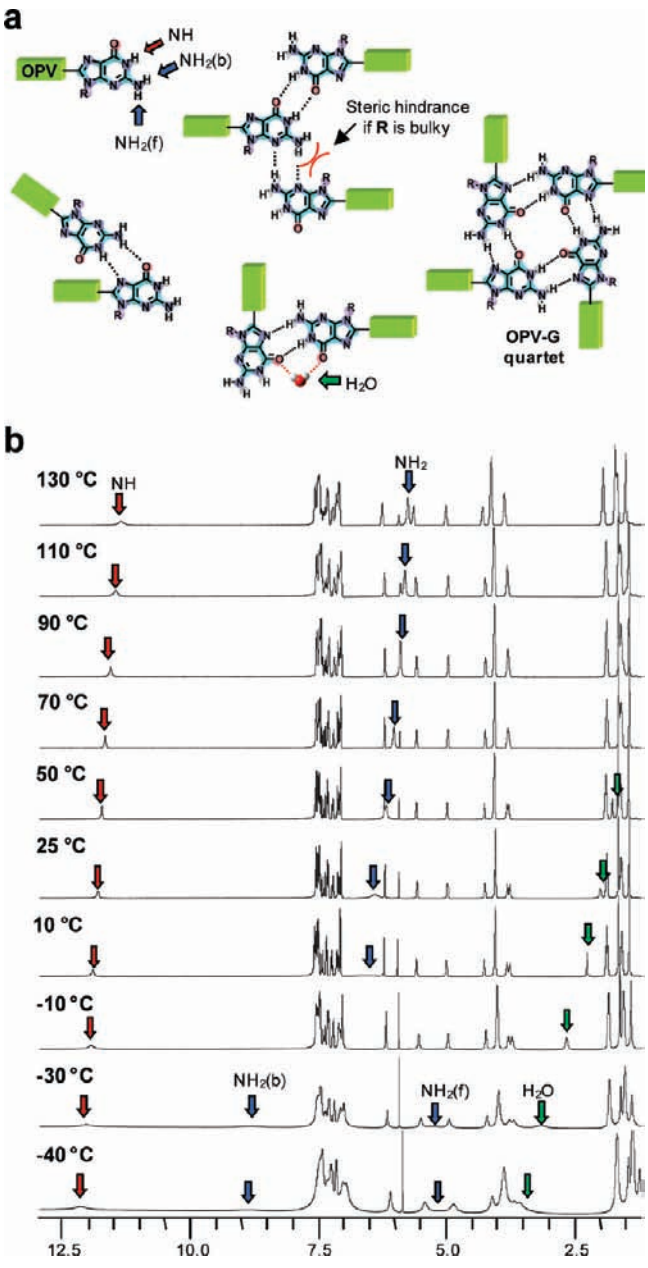

Figure 2. (a) Different modes of self-association of the OPV-G molecules by pairs of hydrogen bonds. When the group R on the guanine is a bulky ribose, as in the case for **OPV-G1** and **OPV-G2**, the formation of the so-called G-ribbon B is prevented by steric hindrance, leading to the preferential formation of cyclic oligomers that eventually form G-quartets. Traces of water can participate in the process of stabilization of these cyclic oligomers by hydrogen-bonding to the carbonyl groups. (b) Portion of the ^{1}H NMR spectra of **OPV-G1** ($CDCl_2CDCl_2$; 10^{-2} M) as a function of the temperature. In less polar solvents or at lower temperatures, both the amide (NH; red arrow) and amine (NH_2; blue arrow) proton signals experience a downfield shift, as a result of a higher participation in hydrogen-bonding. The water signal is indicated by a green arrow.

formation of hydrogen-bonded G-ribbons by steric blockage of the NH_2(f) proton (see Figure 2a).[16,31] As a result, the formation of circular G-quartets, where the NH_2(f) proton does not participate in hydrogen-bonding, must become dominant at high self-association degrees (see Figure 2a). The stabilization of quartet structures is evidenced, as has been described before,[31] in the evolution of the NH_2 proton signal upon cooling **OPV-G1** or **OPV-G2** solutions in, for instance, $CDCl_2CDCl_2$ (Figure 2c; see also Figure S3 for **G1**). At high temperatures these protons are equivalent due to fast spinning around the C−N bond and therefore appear as a broad singlet between 6.5 and 5.5 ppm. Lowering the temperature below 25 °C, however, causes a considerable broadening of this signal that then, below 0 °C, splits into two signals as the quartet is stabilized and the two amino protons exchange slowly on the NMR time scale. The downfield-shifted signal at approximately 9 ppm is assigned to the hydrogen-bonded proton in the quartet (NH_2(b)), whereas the signal around 5 ppm belongs to the "free", solvent-exposed amino proton (NH_2(f)).

It is also interesting to see that, parallel to these changes observed when decreasing the temperature, the water signal[32] undergoes a considerable downfield shift (from 1.5 to 3.5 ppm; green arrow in Figure 2c). This seems to indicate, as has been proposed before,[33] that water molecules are involved in the stabilization of "closed" oligomers, which eventually lead to cyclic tetramers, by hydrogen-bonding to the guanine carbonyl groups (see Figure 2a).

The aggregation of these compounds in nonpolar solvents at lower concentrations (4×10^{-4}−10^{-5} M) was also studied by circular dichroism (CD), absorption, and fluorescence spectroscopic techniques (Figure S4). The combined results indicate that, at the concentrations employed in these experiments, these OPV-G molecules, including **OPV-G3**, do not show a strong tendency to $\pi-\pi$ stack in ordered aggregates. For instance, only a small positive Cotton effect with a zero-crossing at the maximum of the OPV absorption (~420 nm) was observed in very apolar solvents as methylcyclohexane or dodecane, indicating that the degree of chiral order is low. This CD signal did not change considerably with the concentration of the sample or the temperature. In addition, the normalized absorption and emission spectra at different concentrations and in different solvents were virtually identical, whereas in temperature-dependent experiments we only observed the typical red shift in the absorption and emission spectra due to planarization of the OPVs, which increases linearly when decreasing the temperature (see Figure S4).

The low degree of aggregation observed in our OPV-G molecules at low concentrations is not entirely surprising in view of the dense substitution of our molecules (especially **OPV-G1** and **OPV-G2**), the low rotational barriers around triple bonds, and the relatively weak and unspecific self-association by pairs of hydrogen bonds, which may give rise to a complex mixture of oligomers in fast exchange. These results contrast with comparable OPV molecules studied previously in our group that can form strong and specific quadruple hydrogen-bonded dimers, which show a large driving force to stack in long helical fibers.[34]

Self-Assembly in the Absence of Cations. Surface Experiments. Scanning Tunneling Microscopy (STM) experiments provided a clearer picture on the self-assembly of our OPV-G molecules in the absence of cations, and the results are consistent with the interpretations drawn from solution experiments. For instance, 10^{-4}−10^{-6} M solutions of **OPV-G3** in 1-phenyloctane or octanoic acid yielded very disordered monolayers in which

(32) The traces of water mainly come from the residual water in the deuterated solvent and are difficult to eliminate totally.
(33) Kotch, F. W.; Sidorov, V.; Lam, Y.-F.; Kayser, K. J.; Li, H.; Kaucher, M. S.; Davis, J. T. *J. Am. Chem. Soc.* **2003**, *125*, 15140–15150.
(34) (a) Schenning, A. P. H. J.; Jonkheijm, P.; Peeters, E.; Meijer, E. W. *J. Am. Chem. Soc.* **2001**, *123*, 409–416. (b) Jonkheijm, P.; van der Schoot, P.; Schenning, A. P. H. J.; Meijer, E. W. *Science* **2006**, *313* (5783), 80–83.

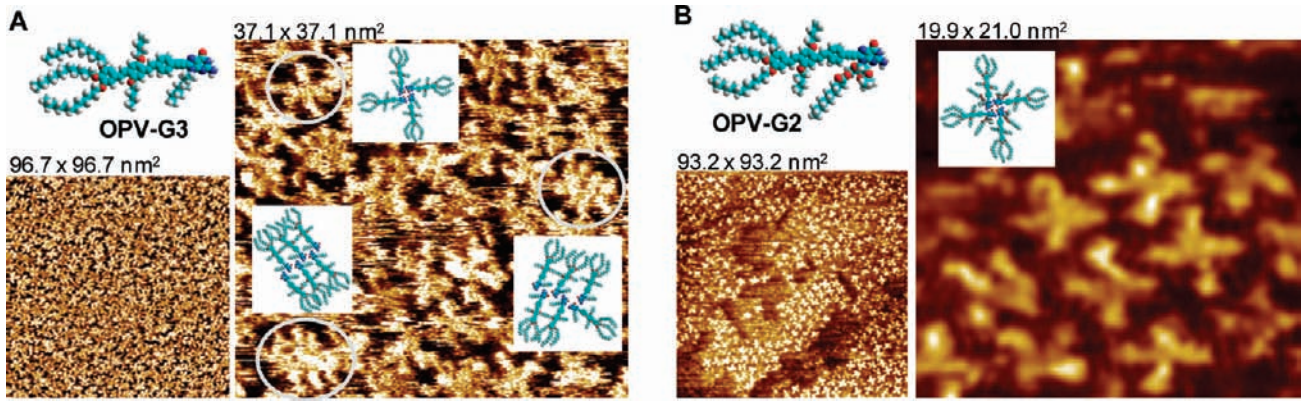

Figure 3. Scanning tunneling microscopy (STM) images at the 1-phenyloctane/HOPG interface of (a) **OPV-G3** (6×10^{-4} M; 20 °C), with tunneling parameters $I_{set} = 0.026$ nA, $V_{set} = -0.680$ V, and (b) **OPV-G2** (7×10^{-6} M; 20 °C), with tunneling parameters $I_{set} = 0.028$ nA, $V_{set} = -0.600$ V. The insets are tentative models of the corresponding features in the STM images.

we could distinguish diverse oligomeric species, such as small ribbons and quartets (Figure 3a). In general, high quality images were difficult to obtain due to the lack of two-dimensional ordering and the rapid reorganization of the adsorbed molecules, as observed in consecutive scans. This mixture of disordered and fast exchanging oligomers contrasts with previous studies on oligothiophene-G molecules connected *via* the 5′-position of the ribose that do show a long-range ordering in G-ribbons.[19c]

Now, when we moved to compound **OPV-G2**, substituted with a guanosine moiety, we found that the morphology of the monolayers is totally different. Despite the two-dimensional ordering is still poor, all **OPV-G2** molecules are mostly assembled in individual quartets on the HOPG surface (Figures 3b and S5), a kind of organization that, to the best of our knowledge, has not been observed before using STM.[35] This divergence in the self-assembly between **OPV-G2** and **OPV-G3**,[36] as previously evidenced in the NMR experiments, agrees with the notion of steric blocking of the NH_2(f) proton by the bulky ribose group, which prevents the formation of G-ribbons and thus stabilizes the circular tetramers.[37]

Self-Assembly in the Presence of Cations. Solution Experiments. The whole supramolecular picture changes dramatically upon complexation of the OPV-G compounds with Na^+ or K^+ salts. The strong affinity of the G-quartet cavity for alkaline cations shifts the equilibrium between these loosely bound hydrogen-bonded species toward the formation of well-defined G-quadruplexes (see Figure 1). In these assemblies, the cation is efficiently coordinated by eight carbonyl groups and is typically positioned between two stacking quartets, whereas the anion is left out at the complex periphery. In organic solvents, lipophilic G derivatives usually assemble into discrete G-quadruplexes (2 to 6 stacked quartets; 8mers to 24mers). The kind of complex obtained is very sensitive to the experimental conditions employed, depending particularly on the nature of the anion or the guanosine derivative employed, as well as on the solvent polarity.[14−17]

In the present study, the complexation of alkaline salts by our OPV-G molecules always produced octamers of D_4-symmetry (D_4-8mers). For example, stirring a 10^{-1} M THF-d_8 solution of **OPV-G1** in the presence of 0.25 equiv of KPF_6 results in the quantitative formation of a D_4-8mer, which reproduces exactly the self-assembly of the bromoguanosine precursor **G1** (Figure S6).[16] As shown in Figure 4a, the ^{1}H NMR spectrum of the D_4-8mer presents characteristic proton signals that differ from the uncomplexed OPV-G species. The amide proton signal becomes sharper and downfield-shifted upon complexation, the amino protons split into two signals (NH_2(b) and NH_2(f)) that become more perceptible at low temperatures, and the signals of the protons on the OPV fragment show a small broadening. Temperature-dependent NMR experiments (Figure 4b) revealed that these 8mers are still stable at temperatures close to the boiling point of the THF-d_8 solvent, and no significant dissociation is detected at, for instance, 50 °C. In this relatively polar solvent, the OPV-G D_4-8mers are, in contrast, very sensitive to the concentration and, as observed for **G1**,[16] dissociation into the uncomplexed OPV-G species takes place upon dilution of the sample until, below 5×10^{-3} M, only uncomplexed OPV-G (mostly in the form of monomeric species or small, loosely bound oligomers) is present in solution (Figure 4c). The two species in equilibrium (8mer and uncomplexed OPV-G) could also be detected in DOSY NMR experiments in THF-d_8 at concentrations between 10^{-1} and 5×10^{-3} M (Figure S7).

The formation of a D_4-symmetric 8mer seems to be general for all the three OPV-G molecules in different conditions. Changes in the nature of the cation (K^+, Na^+) or the anion (PF_6^-, BPh_4^-, I^-, $MeDNP^-$ (4-methyl-2,6-dinitrophenolate)) had virtually no influence on the self-assembly of our OPV-G compounds. Aggregation is therefore limited to octameric assemblies in all the solvents we studied (THF-d_8, $CDCl_3$, $CDCl_2CDCl_2$, toluene-d_8, or cyclohexane-d_{12}).[38]

(35) Hydrogen-bonded networks of quartets of pristine guanines have, however, been reported before. See: Otero, R.; Schöck, M.; Molina, L. M.; Lægsgaard, E.; Stensgaard, I.; Hammer, B.; Besenbacher, F. *Angew. Chem., Int. Ed.* **2005**, *44*, 2270–2275.

(36) The tri(dodecyloxy)benzene wedge of compounds **OPV-G2** and **OPV-G3** is usually important to obtain adsorbed monolayers, and therefore compound **OPV-G1** was not analyzed.

(37) It is interesting to note that neither the controlled addition of sodium or potassium salts to these 1-phenyloctane or octanoic acid solutions nor the analysis of previously assembled OPV-G 8mers led to the observation of adsorbed molecules. This result is not entirely surprising in view of the increase in height of the complexed OPV-G assemblies, which would lead to longer tip−substrate distances.

(38) It has been recently demonstrated that the growth of these G-quadruplex assemblies, up to a 12mer or a 16mer, can be finely controlled in organic media by a subtle interplay between anion−complex (see refs 14,16) and anion−solvent interactions (see refs 15b,16). In particular, more polar solvents, such as acetone or acetonitrile, can stabilize more efficiently the anion in solution and tend to lead to higher complexes. Unfortunately, our OPV-G molecules were not sufficiently soluble in those solvents.

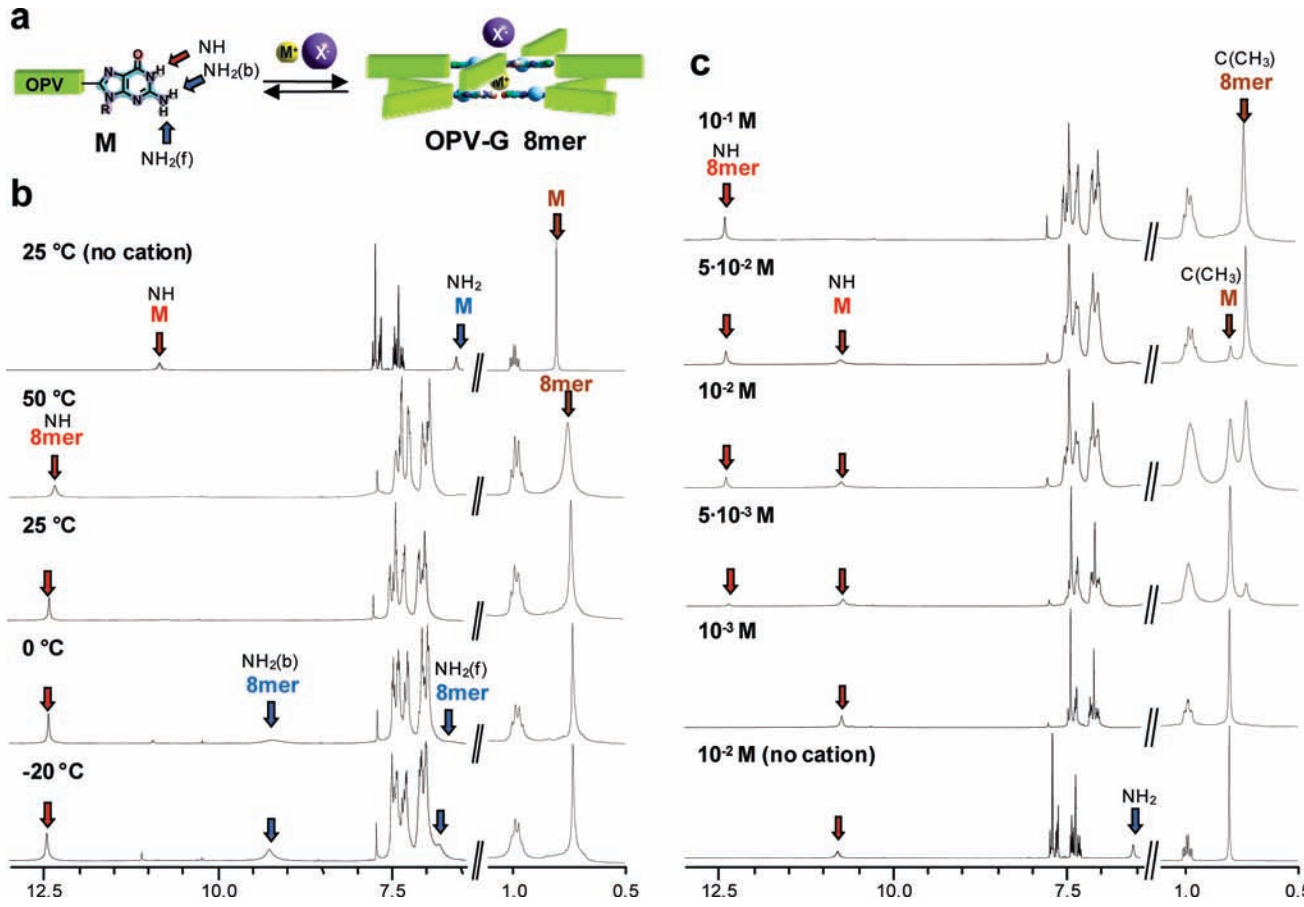

Figure 4. (a) Schematic representation of the equilibrium between uncomplexed OPV-G (**M**) and the D_4-symmetric octamer (**8mer**) in the presence of potassium salts. (b, c) Changes in the NH/NH_2 and *tert*-butyl regions of the ^{1}H NMR spectra of **OPV-G1** in THF-d_8 in the presence of 0.25 equiv of KPF_6 as a function of (b) the temperature ([**OPV-G1**] = 10^{-1} M) or (c) the **OPV-G1** concentration (T = 25 °C).

However, we noticed that reducing the solvent polarity had an enormous effect on the stability of the octameric nanoobjects formed toward temperature or concentration changes. For instance, ^{1}H NMR experiments in toluene or cyclohexane solutions revealed that they can be heated to 75 °C (Figure 5a) or diluted up to 10^{-4} M (Figure 5b) without any evidence of significant dissociation. In agreement with these observations, in DOSY NMR experiments at different concentrations we detected the 8mer complex as the only species in solution.

The persistence of the OPV-G 8mer structures in diluted apolar solutions allowed us to overlap the NMR studies (up to 10^{-4} M) with spectroscopic studies (4×10^{-4}–10^{-5} M), using CD, absorption, and emission techniques. Compared to the uncomplexed oligomers, **OPV-G2** and **OPV-G3** 8mers display distinct features that originate from the well-defined stacking arrangement of the chromophores. As shown in Figure 6a, complexation brings about a small red shift and tailing of the OPV absorption band, as well as a 2- to 3-fold enhancement and bathochromic shift of the fluorescence emission (see also Figure S8). For example, the **OPV-G2**/**OPV-G3** fluorescence quantum yields increase from 0.32/0.37 in the samples without cations to 0.84/0.81 in their respective $KBPh_4$-8mers in toluene. A similar trend was observed in methylcyclohexane, though the quantum yield values derived were somewhat lower for both the monomeric and octameric **OPV-G2**/**OPV-G3** systems (0.30/0.29 and 0.68/0.72, respectively). Moreover, the self-assembled nanostructures exhibit a negative Cotton effect with a zero-crossing ($\lambda_{z\text{-}c}$) at the OPV absorption maximum, when compared to the uncomplexed oligomers, which has a similar shape for both **OPV-G2** and **OPV-G3** despite the different nature of the chiral substituents at the G unit. It is interesting to note that related oligothiophene-G D_4-symmetric octamers, where the oligomer was attached to the 5′-position of the G ribose, showed a similar negative Cotton effect.[19c]

Further spectroscopic studies confirmed the outstanding stability of these G-quadruplex nanoparticles in nonpolar media. For instance, the 8mers can be diluted by a factor of 40 (up to 10^{-5} M) without any change in the CD, absorption, or emission spectrum (Figure 6b). Furthermore, the diluted (4×10^{-5}–10^{-5} M) solutions can be heated up to 75 °C without any other absorption change than the typical red shift assigned to the planarization of the OPV units (Figure 6c). Returning to 20 °C after these heating–cooling cycles resulted in identical absorption, fluorescence, and CD spectra compared to those of freshly prepared samples. Even the addition of small amounts (<5% v/v) of polar additives, such as diisopropylethylamine or *N*-methyl-2-pyrrolidinone, produced no spectroscopic change. The G-quadruplex particles were, however, immediately dissociated upon dilution in a more polar solvent, such as THF (Figure 6b), which is consistent with the results obtained in the NMR experiments (see Figure 4c).

These results suggest that the π-conjugated oligomers are strongly maintained in a well-defined chiral arrangement within the complex, which must be determined by the G-K^+ coordination and steric interactions between the chiral side groups on the G unit, and further transmitted to the OPVs through the rigid ethynyl spacer. The molecular models[39] of the OPV-G 8mers (Figure 7), obtained by using some geometrical param-

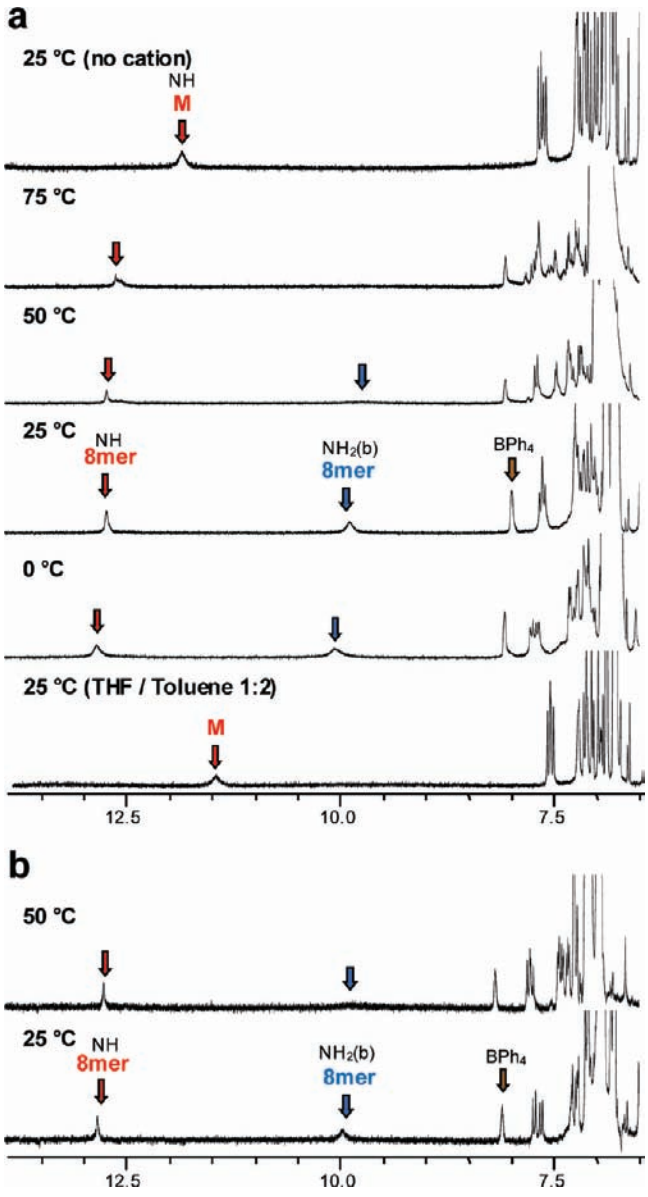

Figure 5. Changes in a region of the ^{1}H NMR spectra of **OPV-G2** in the presence of 0.25 equiv of $KBPh_4$ in toluene-d_8 as a function of the temperature at an OPV-G concentration of (a) 10^{-3} M or (b) 10^{-4} M. For comparison, we are also showing the spectra of **OPV-G2** in the absence of cation and in a THF-d_8−toluene-d_8 mixture, where only uncomplexed species are present (**M**). The amide (NH) and amine (NH_2(b)) proton signals are indicated by red and blue arrows, respectively. The integration of the signal of the protons of complexed $KBPh_4$ (brown arrow) supports the formation of a 1:8 complex.

eters from the reported crystal structures of related G-quadruplexes,[14a,16,31] indicated that the OPVs are positioned at a suitable distance for $\pi-\pi$ stacking (3.3 Å), but their π-conjugated surfaces overlap only partially, due to the *ca.* 30° angle imposed by the two quartets upon K^+ complexation. Particle dimensions of ~1.5−2.0 nm high[40] and 8.5 nm wide

(39) Structural modeling was performed using the MM$^+$ method implemented on the Hyperchem 8.03 software package (Hypercube, Inc.) for Windows. Some of the geometrical parameters (quartet−quartet distance, position of the cation, relative orientation of quartets) were kept within the values observed in the crystal structures reported in the literature (see refs 14a,16,31). In these models, the anion was positioned on top of one of the quartets, since this leads to the shorter cation−anion distance due to the dense peripheral crowding.

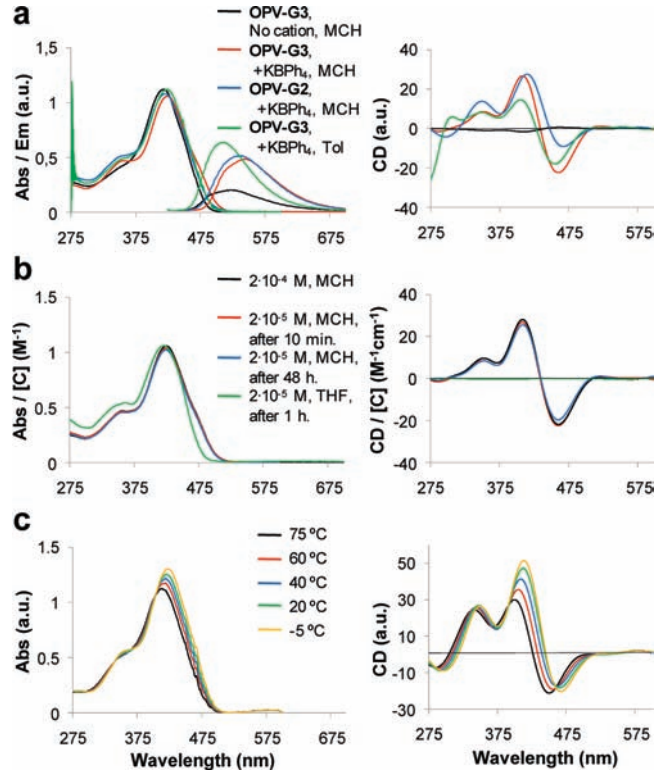

Figure 6. Absorption, emission (λ_{exc} = 420 nm) and circular dichroism (CD) spectra of (a) **OPV-G3** or **OPV-G2**, in the absence or in the presence of 0.25 equiv of $KBPh_4$, in toluene or MCH, as indicated in the figure legends ([OPV-G] = 4×10^{-5} M; 20 °C), (b) **OPV-G3** in MCH before and after 10-fold dilution with MCH or THF (20 °C), or (c) **OPV-G3** as a function of the temperature (MCH; 4×10^{-5} M).

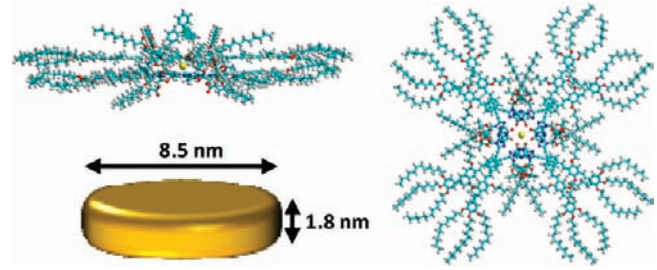

Figure 7. Top and side views of the D_4-8mer model of **OPV-G2** with $KBPh_4$. The BPh_4^- anion (only shown in the side view) has been arbitrarily positioned on top of the complex, since it leads to the shorter cation−anion distance. Complex dimensions were derived from these models.[40]

were derived from these models taking into account the alkyl tails and the anion.

Self-Assembly in the Presence of Cations. Solid-State X-ray Diffraction Experiments. X-ray diffraction (XRD) studies were conducted at room temperature on bulk samples of **OPV-G1**, **OPV-G2**, and **OPV-G3**, as well as of their respective Na^+- or K^+-D_4-8mers. In the wide angle region, only **OPV-G3** samples showed a diffraction maximum at 0.35 nm, corresponding to the $\pi-\pi$ stacking distance, which is sharper and more intense in the complexes, indicating that the addition of a cation favors the stacking (see Figure S9). The samples of guanosine-OPVs **OPV-G1** and **OPV-G2**, however, did not display this

(40) Small variations on the calculated particle height mainly come from the size of the anion employed and also from the conformation of the substituents on the G unit and the OPV tri(dodecyloxy)benzene wedge.

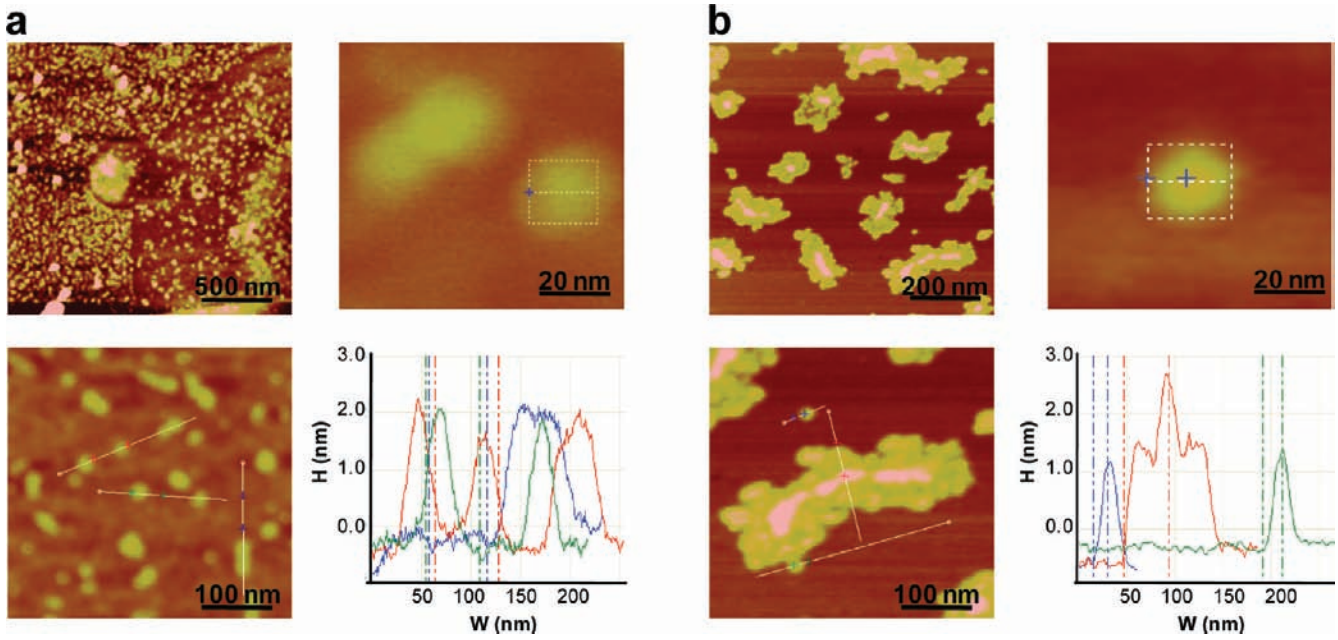

Figure 8. AFM images of the [**OPV-G3**]$_8$-KMeDNP nanoparticles deposited from 10^{-5} M solutions in toluene on (a) graphite or (b) mica surfaces.

maximum, which demonstrates the detrimental effect of the pending bulky ribose on the stacking. The diffraction patterns of the samples containing **OPV-G2** and **OPV-G3** exhibit as well a diffuse halo corresponding to ~0.45 nm, which is the typical distance between the molten long alkyl tails in liquid crystals (Figure S9).[41]

Self-Assembly in the Presence of Cations. AFM Surface Experiments. To confirm the integrity and uniformity of the **OPV-G2** and **OPV-G3** complexes formed in the presence of K^+ salts, we deposited diluted (10^{-4}−10^{-5} M) solutions in apolar solvents such as toluene or methylcyclohexane over graphite or mica surfaces and, after solvent evaporation, imaged the self-assembled nanoobjects by atomic force microscopy (AFM; Figure 8).

The atomic force micrographs of drop-casted **OPV-G2** and **OPV-G3** D_4-8mer solutions show nanoparticles whose dimensions, considering the convolution with a tip of radius of curvature of 15−20 nm (10 ± 5 nm width and 1.8 ± 0.4 nm height),[42] nicely match those estimated for the OPV-G D_4-8mers (8.5 nm width and 1.8 nm height). On graphite (Figures 8a and S10a), we could generally observe the individual nanoparticles at low sample concentrations,[43] together with some larger objects probably formed by further aggregation of these particles. On mica surfaces (Figures 8b and S10b), the OPV-G 8mers aggregate into mono- and bilayers with a height of 1.8 ± 0.4 nm and 3.2 ± 0.4 nm, respectively, and we could only see a few isolated nanoparticles. In the absence of potassium salts, we observed in contrast very different features. For instance, **OPV-G3** molecules formed mono- and bilayers on graphite, together with larger objects, but the characteristic 8mer nanoparticles were not detected.

We think that the degree of nanoparticle aggregation observed on both surfaces is simply a result of the interaction of the lipophilic alkyl tails with the surface, which provides the particles with some mobility upon physisorption. This interaction is much lower on mica than on graphite, and therefore, the nanoparticles can rearrange to a certain extent and form aggregates during solvent evaporation. In contrast, on graphite the 8mers display a much reduced mobility. Aside from this nanoparticle aggregation phenomenon, presumably occurring upon sample drying, we never detected the formation of elongated, fiber-like structures that could have been formed by further aggregation of OPV-G quartets. This fact underscores the uniformity and supramolecular identity of our octameric OPV-G particles.

Conclusions

Molecular self-assembly is a powerful tool that may be used to construct, in a bottom-up approach, persistent and monodisperse nanoobjects where a discrete number of functional molecules are organized in a well-defined arrangement. For such a goal, one must be able to modulate the interplay between multiple noncovalent interactions so that they work in concert to impart stability to the assemblies and, at the same time, limit their growth to a certain extent. We have shown that the special characteristics of G-quadruplex self-assembly meet these requirements and, in certain conditions, allow the supramolecular synthesis of disk-shaped ONPs comprising exactly eight π-conjugated molecules. The rigid, chirally tilted arrangement of the OPVs within the octameric complexes results in negative Cotton effects, bathochromic shifts of the absorption and emission bands, and a 2- to 3-fold enhancement of the fluorescence emission. These features are also characteristic of larger ONPs (>25 nm), typically produced by reprecipitation methods,[4,7] that show size-dependent emission quantum yields, but for which particle size and chromophore organization is more difficult to control. Future research will be directed to gradually increasing the size (particularly the height) of these self-assembled nanoobjects,[38] which might

(41) However, optically polarized microscopy experiments revealed that none of the OPV-G compounds, in the presence or absence of Na^+/K^+ cations, displayed liquid crystalline behavior in the temperature range 20−220 °C.
(42) Bustamante, C.; Vesenka, J.; Tang, C. L.; Rees, W.; Guthold, M.; Keller, R. *Biochemistry* **1992**, *31*, 22–26.
(43) More concentrated samples led to thick layers where individual nanoparticles could not be observed. However, we expect that these layers consist of assembled nanoparticles.

result in a progressive fluorescence enhancement as a function of the number of stacked quartets, as well as to the study of the dynamics of these systems.

Acknowledgment. The authors are grateful for the financial support from the Council for the Chemical Sciences of The Netherlands Organization for Scientific Research (CW-NWO) and the EURYI scheme. D.G.R. and R.M.-R. would like to acknowledge a Marie Curie Intraeuropean Fellowship. The authors would also like to thank K. U. Leuven (GOA), the Belgian Federal Science Policy Office through IAP-6/27 and the Fund for Scientific Research-Flanders (FWO). I.D.C. thanks the Institute for the Promotion of Innovation by Science and Technology in Flanders (IWT).

Supporting Information Available: Experimental section, synthetic procedures, characterization data, and some selected supplementary figures (Figures S1−S10). This material is available free of charge via the Internet at http://pubs.acs.org.

JA908537K